IEEE Access
Multidisciplinary | Rapid Review | Open Access Journal

Received September 25, 2019, accepted October 10, 2019, date of publication October 23, 2019,
date of current version November 22, 2019.

Digital Object Identifier 10.1109/ACCESS.2019.2949099

A Novel Advanced Traction Power Supply System Based on Modular Multilevel Converter

XIAOQIONG HE[1,2], (Member, IEEE), JUN PENG[1], (Student Member, IEEE), PENGCHENG HAN[1], (Student Member, IEEE), ZI LIU[1], SHIBIN GAO[1,2], AND PENG WANG[3], (Fellow, IEEE)

[1]School of Electrical Engineering, Southwest Jiaotong University, Chengdu 611756, China
[2]National Rail Transit Electrification and Automation Engineering Technique Research Center, Southwest Jiaotong University, Chengdu 611756, China
[3]School of Electrical and Electronic Engineering, Nanyang Technological University, Singapore 639798

Corresponding author: Pengcheng Han (birdhpc@my.swjtu.edu.cn)

This work was supported by the Sichuan Science and Technology Project under Grant 2019YJ0241.

ABSTRACT Due to the attractive advantages such as modularity, scalability and excellent power quality of modular multilevel converter (MMC), converters based on MMC could be a promising alternative solution for traction transformer. A novel MMC-based advanced co-phase traction power supply system is proposed in this paper to solve power quality issues and eliminate the neutral sections in the traditional traction power supply system. And in the proposed system, a DC power transmission system is designed, which provides convenient access for distributed energies benefiting the utilization of the natural resources such as solar energy and wind energy along railways. In order to ensure the normal operation of the proposed system, nearest-level modulation considering voltage balancing is designed for MMCs. The mathematic model three-phase MMC-based rectifier is derived in detail. Based on the mathematic model, dual current-loop control is designed for the rectifier. Besides, the parallel operating traction substations suffer circulating current issue. A droop control combining with double closed-loop control is designed to deal with the problem. The correctness and feasibility of the system and its modulation and control strategies is verified through simulation and a small-scale experiment.

INDEX TERMS Electrified railway, traction power supply system, modular multilevel converter (MMC), three-phase rectifier, single-phase inverter.

I. INTRODUCTION

The traditional traction power supply system that adopts a step-down transformer to feed two strictly isolated feeders is widely used in AC electrified railway system [1]–[5]. But it faces daunting challenges such as power quality issues, power supply ability, and problems caused by neutral sections. Co-phase traction power supply system is proposed to solve power issues and eliminate neutral sections in the substation [2], [3]. Various forms of co-phase power supply systems have been developed. But the neutral sections between the substations still exist [3], [4]. In order to link all the catenaries of any different substations, the advanced co-phase traction power supply system is proposed [5]. The neutral sections are completely eliminated in this system, and the system capacity can be configured as needed. But it is based on diode clamped multilevel converters where with the increase of the number of levels, the complexity of the circuit increases sharply. Therefore, the system is hard to adapt to the application of high-power occasions. The modular multilevel converter (MMC) is more applicable in high-power conversion for its higher modularity, lower output THD, and higher voltage scalability.

In 2003, Mraquardt *et al.* of the Bundeswehr University in Munich, Germany, for the first time proposed MMC, which became the most widely studied and used multilevel converter structure. As its perfect match with high-power applications, a large number of theoretical researches and engineering applications have been carried out in the field. As the basic power unit of MMC, sub-module (SM) has a direct impact on the output characteristics of MMC. Half-bridge sub-module (HBSM) and Full-bridge sub-module (FBSM) are the most widely adopted SM structure of MMC [6]. Compared with HBSM, the number of power devices used in FBSM is twice

The associate editor coordinating the review of this manuscript and approving it for publication was N. Prabaharan.

that of HBSM, which increases the losses and investment of the converter. Besides, converters adopt HBSM occupy fewer hardware resources in the control system. SMs of many other structures have also been proposed according to different application requirements such as high efficiency, dc-fault current blocking, and smaller capacitor voltage ripple [7], [8].

Modulation technology is another key technology of MMC. At present, there are mainly two types of modulation methods for MMC, i.e., staircase modulation and pulse width modulation (PWM). The output voltage of PWM has a better quality due to its higher switching frequency, more suitable for medium-voltage applications [9]. Nearest-level modulation (NLM) is the most popular realization of staircase modulation. Compared with PWM, the switching frequency of NLM is lower, so it has lower power losses and occupies fewer hardware resources. However, the quality of the output voltage of NLM is poor, so it is recommended for high-voltage applications as the level number is large enough to ensure the power quality [10]. A switching state smooth transition based discrete-time NLM strategy is proposed for MMCs with a small number of SM to operate in low frequency which can guarantee a significant reduction of the unnecessary switching actions over the full modulation index range [11]. Some modified NLM strategies are proposed to increase the output level from N to 2N+1 so that NLM can be applied to MMC with fewer SMs [10], [12]. A combination of NLM and PWM is proposed in [9], which inherits the advantages of both NLM and PWM. Improved PWM strategies are also proposed to achieve low power losses and the balance of SM capacitor voltage [13], [14].

In order to ensure MMC works in the desired state, the control system is required to achieve objectives such as SM capacitor voltage control, circulating current control, etc. A generalized mathematical model for MMC in HVDC applications under balanced and unbalanced grid conditions is presented in [15]. According to the model, a dual-current control scheme with positive and negative sequence current controllers is applied. An advanced dual current control method without PLL is proposed in [16]. Simplified model predictive control methods that can reduce the computational burden have been achieved in different ways [17]–[19]. A novel fault-tolerant modulation and control strategy is proposed for MMC in medium voltage applications providing optimum performances under healthy conditions and minimum performance degradation after SM failures [20]. Reference [21] presents a new voltage-balancing control technique with fault detection and fault-tolerant control capability where the need for measuring SM capacitor voltages is eliminated. The circulating current of MMC is mainly composed of even-harmonics such as second harmonic. A circulating current suppression method based on even-harmonics repetitive control scheme is presented in [22]. A novel circulating current suppressing strategy based on virtual impedance sliding mode control (VI-SMC-CCS) is proposed in [23]. Reference [24] applies model predictive control into circulating current suppression.

There have been some studies on applying MMC to electrified railways. MMC-based RPC and its control strategy have attracted much attention [25]–[27], which aims to solve the power quality issues of the traction power supply system. MMC-based co-phase traction power supply system is presented in [3], where the APC is implemented by using a three-phase MMC. But in these applications, only power quality issues can be solved, the neutral sections still remain. Therefore, it is of great significance to research on how to replace the traditional traction transformer with MMC-based power converters [28].

The main contribution of this paper is that a novel MMC-based advanced co-phase traction power supply system with a DC-bus is proposed, the control and modulation strategies are designed to ensure the normal operation of the proposed system. In the proposed MMC-based advanced co-phase traction power supply system, not only neutral sections can be completely eliminated and power quality issues can be thoroughly solved, but also a port for the convenient access of distributed energies such as solar energy, wind energy, and energy storage system is reserved. The modulation strategy considering SM voltage balancing, control strategies for MMC-based rectifier and inverters are designed in this paper, which guarantee the normal operation of the proposed system.

The rest of this paper is organized as follows. In Section II, the configuration, parameter design and modulation strategy of the proposed MMC-based advanced traction power supply system are introduced. The whole control system is designed in Section III, where the dual current-loop control strategy based on the mathematic model of the three-phase MMC-based rectifier and a control strategy combining double closed-loop control and droop control for the single-phase MMC-based inverter are designed separately. On the basis of theoretical analysis, simulation results are given to validate the proposed system in Section VI. Experiment results based on a small experimental prototype are given in Section V to further verify the proposed system with its control and modulation strategies. Conclusions are summarized in Section VI.

II. A NOVEL MMC-BASED ADVANCED TRACTION POWER SUPPLY SYSTEM

A. CONFIGURATION OF THE NOVEL MMC-BASED ADVANCED TRACTION POWER SUPPLY SYSTEM

The novel MMC-based advanced co-phase traction power supply system proposed in this paper is illustrated in Fig. 1. It mainly consists of a connecting transformer, a three-phase MMC-based rectifier, a DC-bus, single-phase MMC-based inverters and single-phase step-down transformers. Three-phase MMC-based rectifier gets power from the three-phase 110kV grid through connecting transformer and then transmits power to all substations through high voltage DC-bus. The single-phase MMC-based inverters in the substation will convert the high-voltage DC into 50Hz AC, and then the AC is reduced to 27.5kV through the single-phase

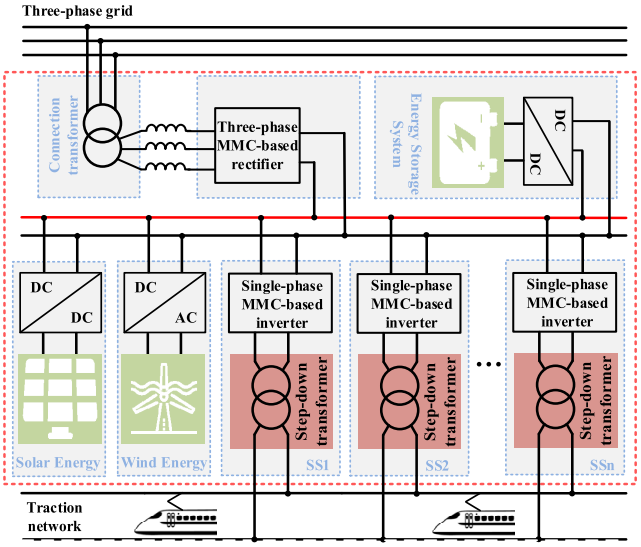

FIGURE 1. Configuration of the novel MMC-based advanced traction power supply system.

step-down transformer to feed the traction network. Because the amplitude, frequency and phase of the output voltage of the inverter in each substation are strictly controlled to be the same, the amplitude, frequency, and phase of the secondary output voltage transformed by the same single-phase step-down transformer should be identical. So that the neutral sections can be canceled, catenaries of all the substations can be linked together. Meanwhile, the converter-based system could also solve the power issues including unbalance, reactive power, and harmonic distortion.

At present, many scholars are working to meet the challenges of developing sustainable and environmentally friendly energy resources. The wide application and fast development of distributed energies have brought new challenges and new possibilities to the traction power supply system. If large-capacity distributed generations such as wind power generation, photovoltaic power generation connected to the traditional AC traction power supply system, the active and reactive power will fluctuate randomly and dramatically, which will cause voltage fluctuation. But the active and reactive power can be controlled independently in the DC system to maintain the stability of the voltage. Due to the existence of the DC-bus, the high-density access and full utilization of distributed energies can be realized in the proposed system, which could bring surprising changes to the traction power supply system. The photovoltaic power generation system and energy storage system can be connected to DC bus through DC-DC converter [29]–[31]. At the same time, the wind power generation system can be connected to DC bus through AC-DC converter.

Compared with the traditional traction power supply system, the newly proposed MMC-based advanced traction power supply system has the advantages as follows.

(1) Solving the inherent problems in the traction power supply system. In the proposed system, power issues such as harmonics, reactive power, and negative sequence will be thoroughly solved. And neutral sections will be completely eliminated, friendly interaction between traction substations and between traction power supply system and power grid can be realized.

(2) High modular design. The number of SM per arm can be adjusted to realize the flexible configuration of system voltage class and power class, which is convenient for system expansion. Besides, SMs are highly replaceable which benefits system maintenance and redundant design.

(3) No requirement of large-capacity capacitors. The DC-side of the MMC does not require large-capacity capacitors or other passive filter components, which avoids surge current caused by short-circuit on the DC-side, improving system reliability, and reducing system cost.

(4) Excellent power quality. Due to the high equivalent switching frequency and output voltage level, the harmonic content of the output voltage is relatively low. So the required filter inductance is small, and even the filter inductance can be canceled, which helps to reduce the system volume.

(5) Convenient access for distributed energies. The proposed system sets a high-voltage DC-bus. On the one hand, the cost of power transmission can be reduced. On the other hand, due to the existence of DC-bus, abundant renewable energies such as wind energy and solar energy along the railway could access easily.

B. STRUCTURE AND PARAMETER DESIGN OF THREE-PHASE TO SINGLE-PHASE MMC CONVERTER

The topology of the three-phase to single-phase MMC is illustrated in Fig.2. Considering the factors of economy, control complexity and efficiency, HBSM is adopted in this paper. The number of SM depends on the voltage class of the SM and DC voltage. The designed DC voltage V_{dc} is 160kV. And the voltage of each SM V_C is designed as 2000V. So the number of SM is n = 160kV/2000V = 80.

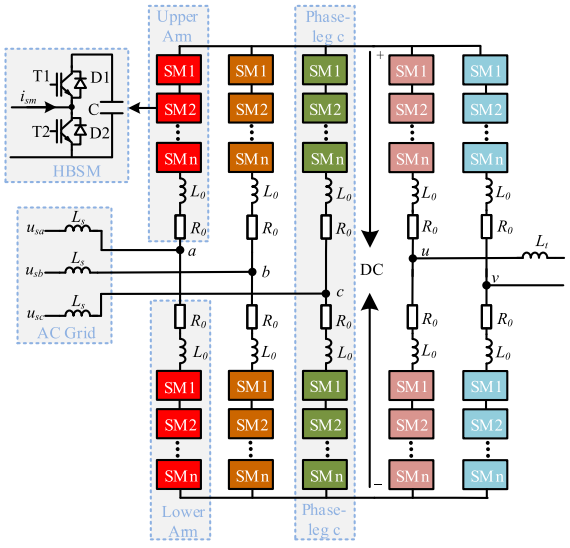

FIGURE 2. The topology of three-phase to single-phase MMC-based converter.

Three-phase MMC-based rectifier is composed of three legs, each of which can be divided into two arms as shown in Fig.2. The bus terminals of each leg are connected to a DC system. The arms connected with the positive terminal name upper arm. Similarly, the arms connected with the negative terminal name lower arm. Each arm consists of a large number of cascaded SMs in series with an inductor L_0. The power losses of each arm are represented by a resistor R_0. The midpoint of each leg is connected to the voltage source through an inductor L_s.

HBSM consists of two IGBTs T1, T2 and a capacitor C as shown in Fig.3. According to the current direction and the switching state of the IGBTs, three working states can be defined. State 1: locked state, where both IGBTs of the SM are turned off. It is used in the startup or fault state. State 2: insert state, where T1 is turned on and T2 is turned off. In this state, the SM could output the capacitor voltage. State 3: bypass state, where T1 is turned off and T2 is turned on. The output voltage of the SM is 0.

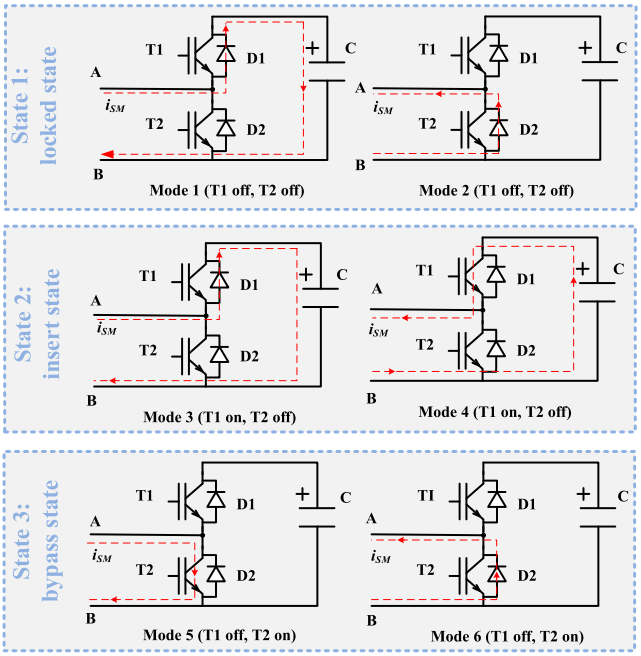

FIGURE 3. Half-bridge SM working status.

C. MMC MODULATION STRATEGY

Since a large number of SMs are series-connected in the proposed MMC-based advanced co-phase traction power supply system, NLM is adopted in this paper. The staircase wave is utilized to approximate the desired sine wave in NLM. So the number of inserted SM in the upper and lower arms is adjusted according to the change of modulation wave.

The number of inserted SM in the upper arm (n_{upper}) and lower arm (n_{lower}) of each phase can be calculated as:

$$\begin{cases} n_{lower} = \dfrac{n}{2} + round(\dfrac{u_{ref}}{U_c}) \\ n_{upper} = \dfrac{n}{2} - round(\dfrac{u_{ref}}{U_c}) \end{cases} \tag{1}$$

where n is the number of SM per arm, u_{ref} is the reference voltage of each phase, U_c is the average capacitor voltage of the SMs, *round*( ) is a function that rounds the nearest integer.

It is easy to find that:

$$n_{upper} + n_{down} = n \tag{2}$$

Equation (2) indicates that the inserted SMs in each phase is always equal to n. It is conducive to maximizing the utilization ratio of the DC voltage and maintaining the stability of the DC voltage. The modulation principle of NLM is shown in Fig.4.

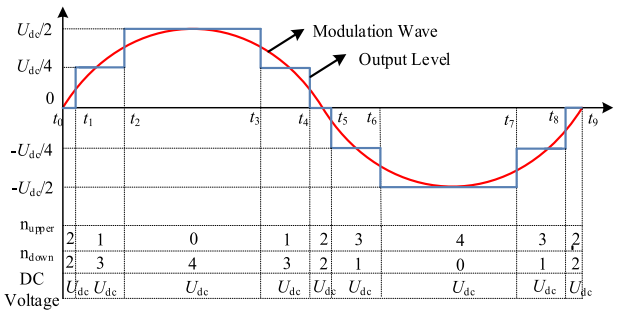

FIGURE 4. NLM modulation algorithm for five-level MMC.

The balance of capacitor voltage is the precondition for the normal operation and control of MMC. In NLM, it is only necessary to ensure the correction of the number of inserted SM in the upper and lower arms. But the SMs actually inserted can be chosen freely. Therefore, the SMs inserted could be chosen according to the arm current direction and SM capacitor voltage, so as to adjust the charging and discharging time of the capacitors. If $i_{sm} > 0$, the capacitors are charging, the lower voltage SMs are selected first. On the contrary, if $i_{sm} < 0$, the capacitors are discharging, the higher voltage SMs are selected first.

III. MMC CONTROL STRATEGY

The overall control system of the proposed MMC-based advanced co-phase traction power supply system includes a three-phase MMC-based rectifier control strategy and a single-phase MMC-based inverter control strategy. The control strategy of the three-phase MMC-based rectifier consists of a DC voltage control and a dual current-loop control, which are used to maintain the stability of DC voltage and ensure the unity power factor operation at AC-side respectively. A control strategy combining double closed-loop control and droop control is designed for the single-phase MMC-based inverter in this paper. The designed control strategy adjusts the output active and reactive power of the inverter to control the phase and amplitude of the inverter output voltages. So that the control strategy can suppress the circulating current between the inverters to ensure safe and stable operation.

A. THREE-PHASE MMC-BASED RECTIFIER CONTROL STRATEGY

Each SM of the MMC can only output two kinds of port voltage, U_C and 0. And each arm is composed of many

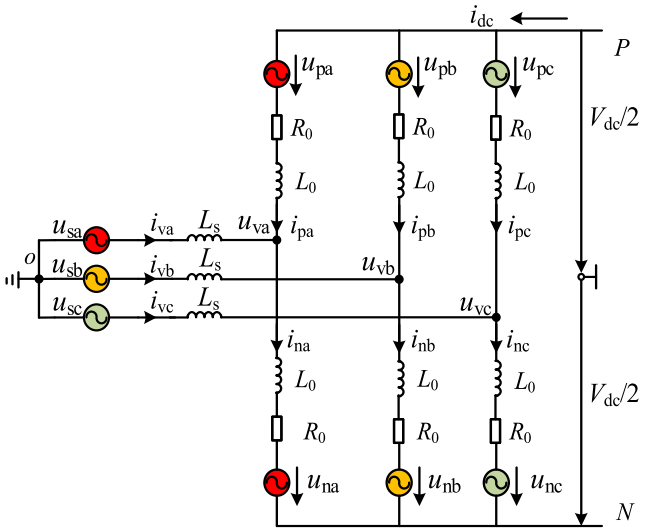

FIGURE 5. Equivalent circuit of the three-phase MMC-based rectifier.

cascaded SMs. So the upper and lower arm of each phase could be equivalent to a controllable voltage source. The equivalent circuit of the three-phase MMC-based rectifier is shown in Fig. 5, where R_0 denotes the equivalent resistance of the arm loss, L_0 denotes arm inductor, L_s denotes filter inductor at AC-side, u_{vj}(j = a,b,c) denotes the fundamental component of the converter output three-phase voltage, u_{sj}(j = a,b,c) denotes the three-phase source voltage, i_{vj}(j = a,b,c) denotes the three-phase current of the AC-side, u_{pj}(j = a,b,c) and u_{nj}(j = a,b,c) denote the equivalent controllable voltage source of the upper arm and lower arm of phase j(j = a,b,c) respectively, i_{pj}(j = a,b,c) and i_{nj}(j = a,b,c) denote the current of upper arm and lower arm of phase j(j = a,b,c) respectively, V_{dc} denotes DC voltage, and i_{dc} denotes the current of the DC-side.

According to Kirchhoff's voltage law, the equation of voltage loop of the upper arm and lower arm can be derived as follows.

$$u_{sj} - L_s\frac{di_{vj}}{dt} + u_{pj} + R_0 i_{pj} + L_0\frac{di_{pj}}{dt} = \frac{V_{dc}}{2} \tag{3}$$

$$u_{sj} - L_s\frac{di_{vj}}{dt} - u_{nj} - R_0 i_{nj} - L_0\frac{di_{nj}}{dt} = -\frac{V_{dc}}{2} \tag{4}$$

Define:

$$u_{diffj} = -\frac{1}{2}(u_{pj} - u_{nj}) = \frac{1}{2}(u_{nj} - u_{pj}) \tag{5}$$

$$u_{comj} = \frac{1}{2}(u_{pj} + u_{nj}) \tag{6}$$

where u_{diffj}(j = a,b,c) and u_{comj}(j = a,b,c) denote differential voltage and common voltage of the upper arm and lower arm respectively.

Define the circulating current of phase j(j = a,b,c) as:

$$i_{cirj} = \frac{1}{2}(i_{pj} + i_{nj}) \tag{7}$$

According to Kirchhoff's current law, the relationship of i_{vj}, i_{pj} and i_{nj} is:

$$i_{vj} = i_{nj} - i_{pj} \tag{8}$$

Based on (3) ∼ (8), the following two equations can be derived easily.

$$u_{sj} = (L_s + \frac{L_0}{2})\frac{di_{vj}}{dt} + \frac{R_0}{2}i_{vj} + u_{diffj} \tag{9}$$

$$L_0\frac{di_{cirj}}{dt} + R_0 i_{cirj} = \frac{V_{dc}}{2} - u_{comj} \tag{10}$$

Define:

$$L = \frac{L_0}{2} + L_s, \quad R = \frac{R_0}{2} \tag{11}$$

Applying (11) to (9) produces the dynamic mathematical model of AC-side in the *abc* frame.

$$\begin{cases} u_{diffa} = u_{sa} - L\dfrac{di_{va}}{dt} - Ri_{va} \\ u_{diffb} = u_{sb} - L\dfrac{di_{vb}}{dt} - Ri_{vb} \\ u_{diffc} = u_{sc} - L\dfrac{di_{vc}}{dt} - Ri_{vc} \end{cases} \tag{12}$$

Through (12), it can be found that the mathematical model of the MMC-based rectifier is similar to that of the traditional rectifier. So theoretically, the control strategy of the traditional rectifier can be applied to the MMC-based rectifier directly. In this paper, classical dual current-loop control strategy is adopted to the MMC-based rectifier. Transform (12) to *dq* frame as:

$$\begin{cases} u_{diffd} = u_{sd} - L\dfrac{di_{vd}}{dt} - Ri_{vd} + \omega L \cdot i_{vq} \\ u_{diffq} = u_{sq} - L\dfrac{di_{vq}}{dt} - Ri_{vq} - \omega L \cdot i_{vd} \end{cases} \tag{13}$$

where the transform matrix is:

$$T_{3s-dq}(\theta) = \frac{2}{3}\begin{bmatrix} \cos\theta & \cos(\theta - \frac{2}{3}\pi) & \cos(\theta + \frac{2}{3}\pi) \\ -\sin\theta & -\sin(\theta - \frac{2}{3}\pi) & -\sin(\theta + \frac{2}{3}\pi) \end{bmatrix} \tag{14}$$

Equation (13) indicates that d-axis component i_{vd} and *q*-axis component i_{vq} of the current are influenced not only by the source voltage u_{sd} and u_{sq}, but also by the current coupling term $\omega \cdot L \cdot i_{vd}$ and $\omega \cdot L \cdot i_{vq}$, so it is necessary to decoupling d-axis component and *q*-axis component of the current. A feed-forward decoupling control strategy is adopted in this paper, and PI controller is used to eliminate the current error, then the current control loop equation of the MMC-based rectifier can be obtained as:

$$\begin{cases} u_{diffd}(s) = u_{sd}(s) + \omega L i_{vq}(s) - \left[i^*_{vd}(s) - i_{vd}(s)\right](k_{p1} + \dfrac{k_{i1}}{s}) \\ u_{diffq}(s) = u_{sq}(s) - \omega L i_{vd}(s) - \left[i^*_{vq}(s) - i_{vq}(s)\right](k_{p2} + \dfrac{k_{i2}}{s}) \end{cases} \tag{15}$$

where i^*_{vd} and i^*_{vq} denote the reference output current of the MMC-based rectifier in *dq* frame, k_{p1}, k_{i1}, k_{p2}, and k_{i2} denote

the proportional and integral parameters of the PI controllers. The current control loop is designed to obtain the preferred differential voltage u_{diffd} and u_{diffq}, so that the output current i_{vd} and i_{vq} can track its reference value i^*_{vd} and i^*_{vq}.

The normal operation of the MMC rectifier requires a stable DC voltage. The active power exchange between the rectifier and the grid will affect the stability of the DC voltage. Therefore, in order to maintain the stability of the DC voltage, the DC voltage control loop is coupled to the d-axis of the dual current -loop control. PI controller is also adopted to eliminate the steady-state error.

$$i^*_{vd} = (k_{p3} + \frac{k_{i3}}{s})(U^*_{dc} - U_{dc}) \tag{16}$$

where k_{p3} and k_{i3} denote the proportional and integral parameters of the PI controller.

Based on the above analysis, d-axis reference current i^*_{vd} is given by the DC voltage control loop. The rectifier is preferred to operate at a unity power factor state, so i^*_{vq} is usually set to 0. Besides, the fundamental frequency active and reactive current i_{vd} and i_{vq} produced by the rectifier are transformed into DC components in dq frame, so they could be obtained by the low-pass filter. The control diagram of the three-phase MMC-based rectifier is shown in Fig. 6.

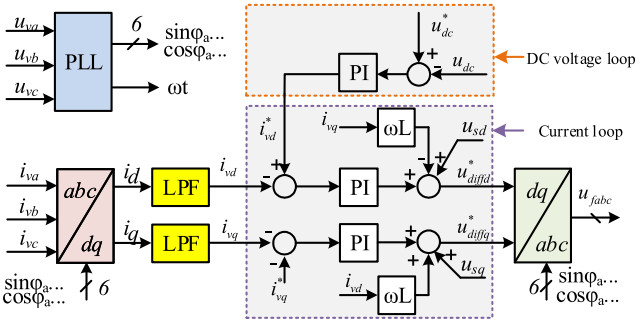

FIGURE 6. Control diagram of the three-phase MMC-based rectifier.

B. SINGLE-PHASE MMC-BASED INVERTER CONTROL STRATEGY

In the proposed MMC-based advanced co-phase traction power supply system, the single-phase inverters are required to operate in parallel. Therefore, the amplitude, frequency, and phase of the output voltage of each inverter have to keep consistent all the time. However, in practical applications, due to various reasons, the amplitude and phase of the voltage output by different inverter will be different, forming a circulating current in the parallel system. The circulating current will not only increase the system losses but also cause the device output power not to be maximized, and could even damage the power device. This paper designs an inverter control strategy combining double closed-loop control and droop control as illustrated in Fig.7. The control of the output voltage of each inverter and the suppression of circulating currents between the inverters are realized through the designed strategy.

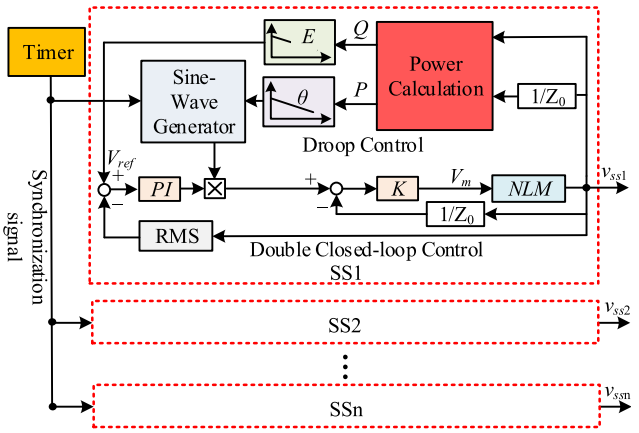

FIGURE 7. Control diagram of the single-phase MMC-based inverter.

The droop control refers to the grid-connected principle of synchronous generators. According to the active power-phase ($P-\theta$) droop characteristic and reactive power-amplitude (Q-V) droop characteristic, the phase and amplitude of the output voltage are controlled respectively. For the system studied in this paper, droop control can adjust the phase and amplitude of the output voltage of the single-phase inverters by detecting the active and reactive power output to the traction network, and the control equations are:

$$\begin{cases} \theta_n = \theta^* - k_\theta \cdot P \\ E_n = E^* - k_E \cdot Q \end{cases} \tag{17}$$

where θ_n and θ^* denote the phase of the output voltage and the reference phase of the output voltage respectively, E_n and E^* denote the amplitude of the output voltage and the reference amplitude of the output voltage respectively, k_θ *and* k_E denote the droop coefficients.

Double closed-loop control is adopted to suppress the influence of load disturbance through a PI controller of the voltage outer loop and a proportional controller of the current inner loop.

IV. SIMULATION VERIFICATION

Referring to the topology of the proposed system shown in Fig.1, a simulation that contains three substations (as shown in Fig.8) is carried out in MATLAB/Simulink. The simulation parameters are listed in Table 1.

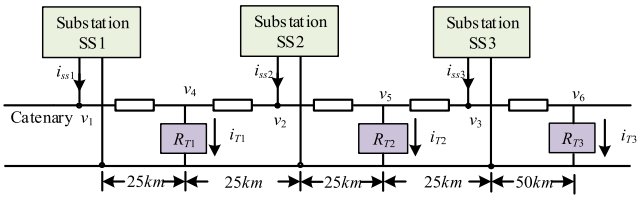

FIGURE 8. Structure of the simulation model.

The simulation process is as follows. Within 0-0.5s, the system is in the start stage, and there is no locomotive load

TABLE 1. Parameters of simulation system.

Parameter	Value
Connecting transformer radio	110kV/110kV
AC inductor	5mF
DC voltage	160kV
SM rated voltage	2000V
SM capacitor	760μF
Arm inductor	70mH
RMS of inverter output voltage	80kV
Filter inductor	320mH
Step-down transformer radio	80kV/27.5kV
locomotive load R_{T1}, R_{T2}, R_{T3}	100Ω
Line impedance	0.14+j0.309Ω/km
simulation step-size	1μs

on the catenary. The locomotive load *RT1*, *RT2*, and *RT3* are gradually put into operation at 0.5s, 0.8s, and 1.2s. Then the locomotive load *RT1*, *RT2*, and *RT3* are gradually removed at 1.6s, 2.0s, 2.4s.

Output voltages v_{ss1}, v_{ss2}, v_{ss3} of the traction substations and the locomotive load voltages v_{RT1}, v_{RT2}, v_{RT3} are shown in Fig.9 and Fig.10. Obviously, the amplitude of each voltage remains almost constant during the whole simulation process, and their RMSs are about 27.5 kV. Even during the switching of various working conditions, the voltages only slightly fluctuate, and can quickly recover and stabilize at around 27.5kV. Due to the locomotive loads gradually increase, the current of the catenary also increases, resulting in an increase in line loss and a slight decrease in the load voltages.

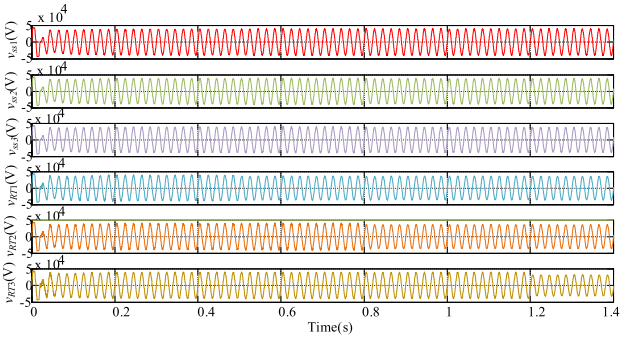

FIGURE 9. Simulation results of traction substation output voltages and locomotive load voltages (0-1.4s).

Output currents i_{ss1}, i_{ss2}, i_{ss3} of the traction substations and the locomotive load currents i_{RT1}, i_{RT2}, i_{RT3} are shown in Fig.11 and Fig.12. When there is no locomotive load on the catenary, the traction substation output currents and load currents are almost 0. When the locomotive load *RT1* is put into operation, the traction substation *SS1* and *SS2* supply power to it, and the two substations each provide half of the energy. When *RT1* and *RT2* are put into operation, the output current of SS1 remains unchanged, the output current of *SS2* increases, and *SS3* is also put into operation. Through the

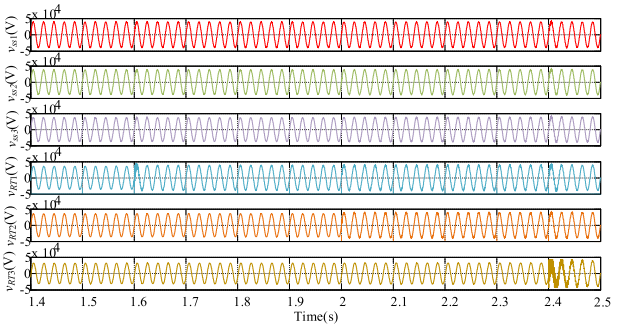

FIGURE 10. Simulation results of traction substation output voltages and locomotive load voltages (1.4-2.5s).

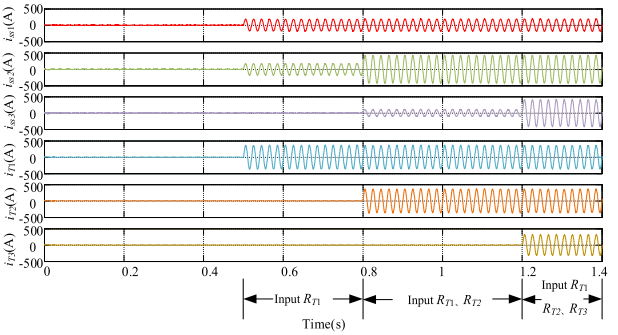

FIGURE 11. Simulation results of traction substations output currents and locomotive load currents (0-1.4s).

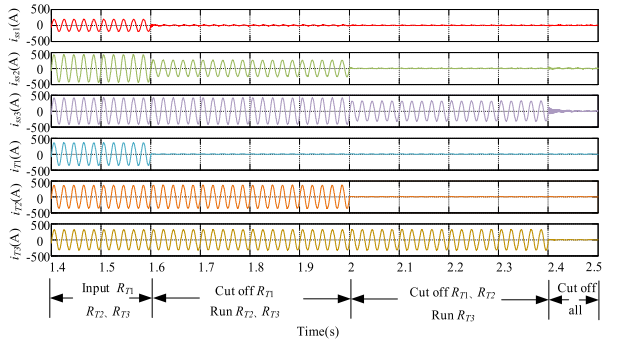

FIGURE 12. Simulation results of traction substations output currents and locomotive load currents (1.4s-2.5s).

value of the substation output currents, it can be found that *SS1* and *SS2* supply power to *RT1*, and *SS2* and *SS3* supply power to *RT2*. When RT3 continues to put into operation, the output current of SS3 increases and the output currents of the other two traction substations remain unchanged, so SS3 supplies power to it. A similar analysis could be obtained when the locomotives are removed gradually. It can be concluded that the impedance distribution of the catenary will affect the source of energy consumed by the load, and the locomotive load current will be provided by the nearest traction substation.

V. EXPERIMENT VERIFICATION

To further verify the proposed novel MMC-based advanced co-phase traction power supply system and its control and modulation strategies, a small experimental prototype is set

up according to the system configuration shown in Fig.13. It is composed of a three-phase MMC-based rectifier, three traction substations with resistance load and a control system mainly composed of FPGA. The main parameters of the system are listed in Table 2.

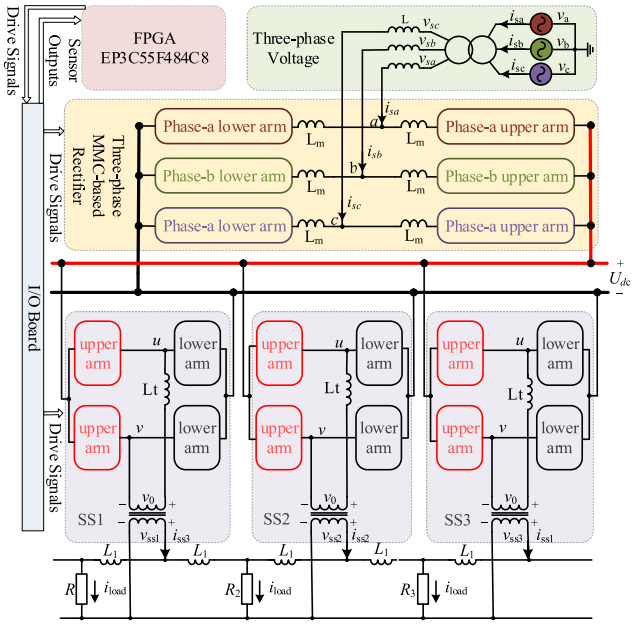

FIGURE 13. Configuration of the prototype.

TABLE 2. Parameters of eixperimental prototype.

Category	Symbol	Parameters	Value
MMC	L_m	Arm inductor	1mH
	V_C	SM rated voltage	60V
	V_{dc}	DC voltage	120V
Rectifier		Step-down transformer radio	380V/60V
		Phase-to-phase voltage	60V
	L	AC-side inductor	5mH
Inverter		RMS of inverter output voltage	80V
	L_t	Filter inductor	10mH
Substation	*R1, R2, R3*	Load	100Ω
	L_l	Line inductor	0.5mH

A. THREE-PHASE MMC-BASED RECTIFIER EXPERIMENT

Firstly, the three-phase MMC-based rectifier experiment is carried out with a 100Ω resistance load. The waveform of the three-phase MMC-based rectifier from the start-up stage to the no-load operation stage and to the loaded operation stage is shown in Fig.14. In the start-up stage, the SM capacitor is charged and the phase current i_{sa} is almost zero. At this period, the converter works in the uncontrolled rectification stage, and the DC voltage has not reached 120 V. In the no-load operation stage, the rectifier control strategy is put into

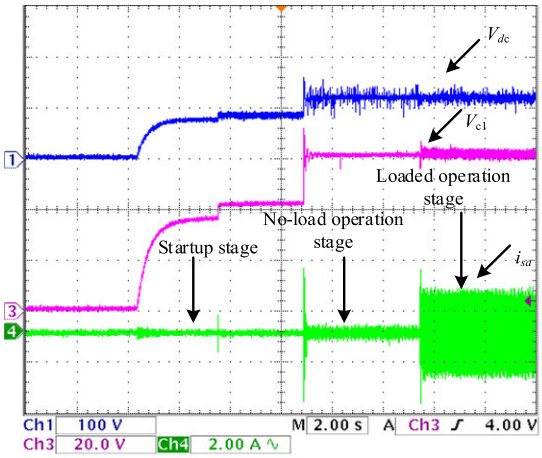

FIGURE 14. Waveforms of three-phase MMC-based rectifier from startup to loading stage. (Ch1: DC voltage V_{dc}, Ch3: SM capacitor voltage V_{c1}, Ch4: AC-side phase current i_{sa}).

operation, the DC-side voltage is stable at about 120V, and the SM capacitor voltage is stable at about 60V which is half of the DC voltage. In other words, the SM capacitor voltage is balanced. From the no-load stage to the loaded stage, the input of load causes an increase of the phase current i_{sa}, but the DC voltage V_{dc} hardly changes.

The steady-state waveform of the three-phase MMC-based rectifier in the loaded operation is shown in Fig.15. At steady state, the AC-side phase voltage v_{sa} and the AC-side phase current i_{sa} are almost in-phase, indicating unity power factor operation of the rectifier. Hence, the effectiveness of the rectifier control strategy is verified.

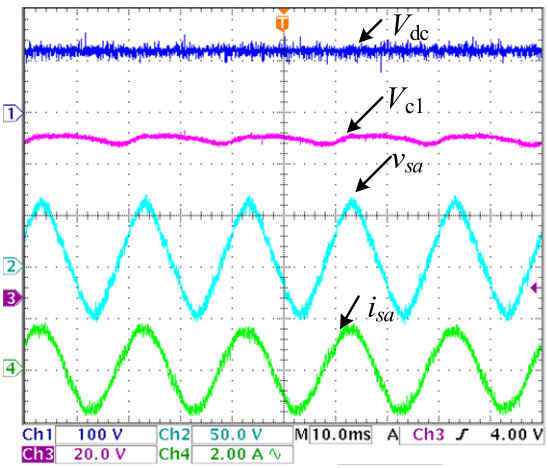

FIGURE 15. Waveforms of three-phase MMC-based rectifier in steady-state. (Ch1: DC voltage V_{dc}, Ch2: AC-side phase voltage v_{sa}, Ch3: SM capacitor voltage V_{c1}, Ch4: AC-side phase current i_{sa}).

B. SINGLE-PHASE MMC-BASED INVERTER EXPERIMENT

Secondly, the single-phase MMC-based inverter is verified, where the DC voltage is set at 120V. The DC source of the experiment is IT6726V.

FIGURE 16. Dynamic waveforms of the advanced co-phase traction power supply system during load increasing.

From the inverter no-load operation to loaded operation, and then to load step-change from 50Ω to 33.3Ω, waveforms of the SM capacitor voltage, output voltage vo and load current iload are shown in Fig.17. From the no load operation to the loaded operation, the load voltage vo can quickly track the reference voltage whose RMS is 80V, frequency is 50Hz as shown in Fig.17(c). When the load step-changes, the load voltage remains stable. The static and dynamic performance of the inverter is verified.

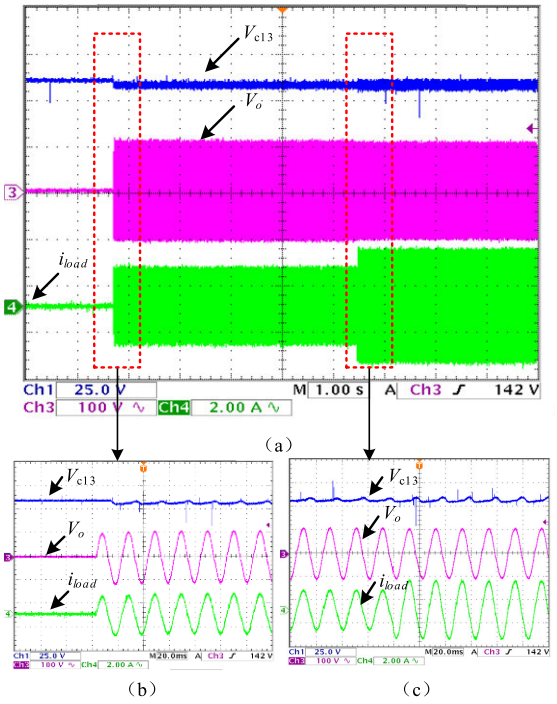

FIGURE 17. Single-phase MMC-based inverter SM capacitor voltage and output voltage v_0 and load current i_{load}. (a) Dynamic waveforms (b) Waveforms of no-load to loaded; (c) Waveforms of load step-change (Ch1: SM capacitor voltage V_{c13}, Ch3: Load voltage v_0, Ch4: Load current i_{load}).

C. THE NOVEL ADVANCED CO-PHASE TRACTION POWER SUPPLY SYSTEM EXPERIMENT

To further verify the feasibility of the whole system proposed in this paper, a small experimental prototype is built according to Fig.13. The experiment of three parallel traction substations is tested.

The dynamic performance when the loads R1, R2, and R3 sequentially input and removed is shown in Fig.18 and Fig.19, respectively. It is easy to find that the amplitude of the output voltage of the inverter always maintains at around 110V regardless of the load change. When the load changes, the DC voltage can still stabilize at 120V, and the SM capacitor voltage can stabilize at about 60V. The stability of the DC voltage, inverter output voltage and the balance of the SM capacitor voltage proof the correctness of the SM capacitor voltage balance control strategy, the rectifier DC voltage control strategy and the inverter control strategy.

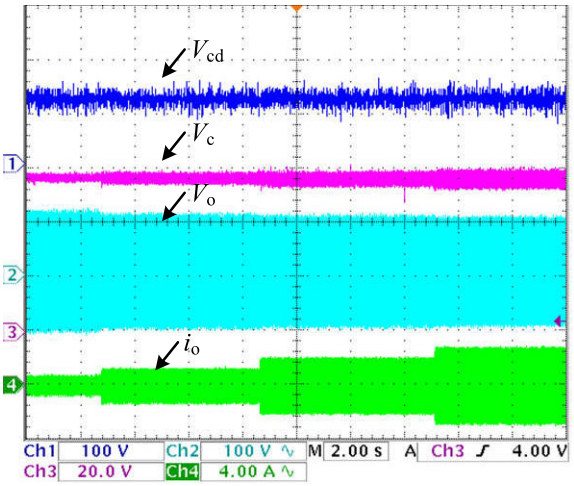

FIGURE 18. Dynamic waveforms of the advanced co-phase traction power supply system during load increasing. (Ch1: DC voltage V_{cd}, Ch2: The primary side voltage of the transformer V_0, Ch3: SM capacitor voltage V_c, Ch4: The primary side current of the transformer i_0).

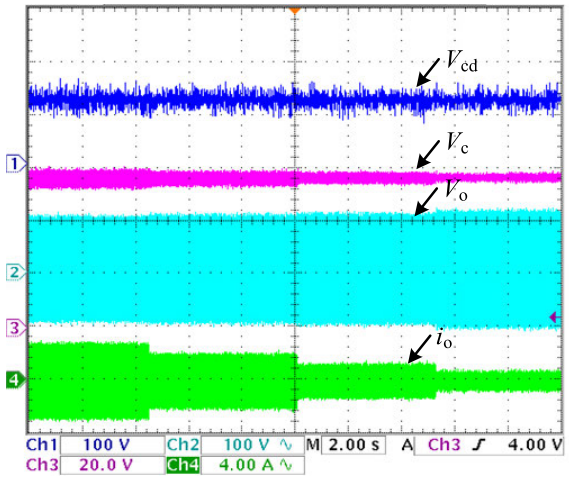

FIGURE 19. Dynamic waveforms of the advanced co-phase traction power supply system during load decreasing (Ch1: DC voltage V_{cd}, Ch2: The primary side voltage of the transformer V_0, Ch3: SM capacitor voltage V_c, Ch4: The primary side current of the transformer i_0).

The steady-state waveform of the advanced co-phase traction power supply system is shown in Fig.20. Obviously, the output voltage and output current of the inverter is sinusoidal. And it is operating in unity power factor state since the output voltage and current are in-phase.

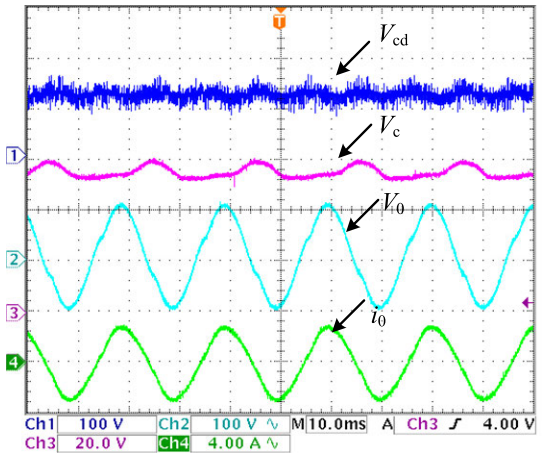

FIGURE 20. Steady-state waveforms of the advanced co-phase traction power supply system (Ch1: DC voltage V_{cd}, Ch2: The primary side voltage of the transformer V_0, Ch3: SM capacitor voltage V_c, Ch4: The primary side current of the transformer i_0).

The output voltage of the traction substation SS1, SS2, SS3 and the output current of SS3 are shown in Fig.21. The phase, amplitude, and frequency of the output voltages of the three traction substations are identical, which indicates that the novel MMC-based traction power supply system proposed in this paper can achieve the integral connection of the traction network.

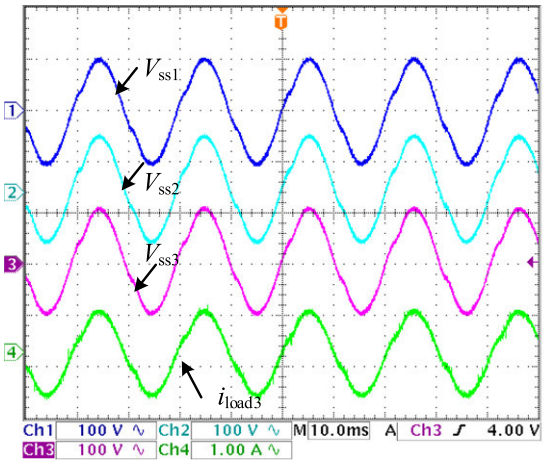

FIGURE 21. Waveforms of the output voltage of SS1, SS2 and SS3 and the output current of SS3 (Ch1: Substation SS1 output voltage V_{ss1}, Ch2: Substation SS2 output voltage V_{ss2}, Ch3: Substation SS3 output voltage V_{ss3}, Ch4: The current of load R3 i_{load3}).

VI. CONCLUSIONS

This paper proposes a novel MMC-based advanced traction power supply system, which is expected to eliminate the neutral sections and solve power quality issues existing in the traditional traction power supply system. A high voltage DC-bus for power transmission is innovatively designed in the proposed system reserving convenient access for distributed energies such as photovoltaic power generation system, energy storage system, and wind power generation system. Due to the specific application occasion, system control and modulation strategies are designed for the three-phase MMC-based rectifier and single-phase MMC-based inverters. Experimental results indicate: 1) the SM capacitor voltage is balanced since SM capacitor voltage balance strategy is considered in NLM. 2) the rectifier could maintain unity power factor operation and the stability of the DC voltage under the designed dual current-loop control associating with DC voltage control. 3) double closed-loop control combining with droop control is designed for the inverters, the system circulating current is suppressed which ensures the normal operation of the parallel traction substations. High modularity, easy voltage scalability, and excellent power quality make the proposed MMC-based advanced traction power supply system a promising alternative for the traditional traction power supply system in the future.

REFERENCES

[1] Q. Li, W. Liu, Z. Shu, S. Xie, and F. Zhou, "Co-phase power supply system for HSR," in *Proc. Int. Power Electron. Conf. (IPEC-Hiroshima-ECCE ASIA)*, Hiroshima, Japan, May 2014, pp. 1050–1053.

[2] Z. Shu, S. Xie, K. Lu, Y. Zhao, X. Nan, D. Qiu, F. Zhou, S. Gao, and Q. Li, "Digital detection, control, and distribution system for co-phase traction power supply application," *IEEE Trans. Ind. Electron.*, vol. 60, no. 5, pp. 1831–1839, May 2013.

[3] Y. Zhao, N. Dai, and B. Wang, "Application of three-phase modular multilevel converter (MMC) in co-phase traction power supply system," in *Proc. IEEE Conf. Expo Transp. Electrific. Asia–Pacific (ITEC Asia–Pacific)*, Beijing, China, Aug./Sep. 2014, pp. 1–6.

[4] M. Chen, Q. Li, C. Roberts, S. Hillmansen, P. Tricoli, N. Zhao, and I. Krastev, "Modelling and performance analysis of advanced combined co-phase traction power supply system in electrified railway," *IET Gener. Transm. Distrib.*, vol. 10, no. 4, pp. 906–916, Mar. 2016.

[5] X. He, Z. Shu, X. Peng, Q. Zhou, Y. Zhou, Q. Zhou, and S. Gao, "Advanced cophase traction power supply system based on three-phase to single-phase converter," *IEEE Trans. Power Electron.*, vol. 29, no. 10, pp. 5323–5333, Oct. 2014.

[6] Z. Shu, M. Liu, L. Zhao, S. Song, Q. Zhou, and X. He, "Predictive harmonic control and its optimal digital implementation for MMC-based active power filter," *IEEE Trans. Ind. Electron.*, vol. 63, no. 8, pp. 5244–5254, Aug. 2016.

[7] M. Lu, J. Hu, R. Zeng, W. Li, and L. Lin, "Imbalance mechanism and balanced control of capacitor voltage for a hybrid modular multilevel converter," *IEEE Trans. Power Electron.*, vol. 33, no. 7, pp. 5686–5696, Jul. 2018.

[8] R. Wang, Z. Li, X. Wen, N. Liu, and X. Wang, "A novel MMC submodule topology with DC fault clearance capability," *IEEE Access*, vol. 7, pp. 96085–96093, 2019.

[9] Y. Wang, C. Hu, R. Ding, L. Xu, C. Fu, and E. Yang, "A nearest level PWM method for the MMC in DC distribution grids," *IEEE Trans. Power Electron.*, vol. 33, no. 11, pp. 9209–9218, Nov. 2018.

[10] L. Lin, Y. Lin, Z. He, Y. Chen, J. Hu, and W. Li, "Improved nearest-level modulation for a modular multilevel converter with a lower submodule number," *IEEE Trans. Power Electron.*, vol. 31, no. 8, pp. 5369–5377, Aug. 2016.

[11] K. Shen, S. Wang, D. Zhao, and G. Zhao, "A discrete-time low-frequency-ratio nearest level modulation strategy for modular multilevel converters with small number of power modules," *IEEE Access*, vol. 7, pp. 25792–25803, 2019.

[12] P. Hu and D. Jiang, "A level-increased nearest level modulation method for modular multilevel converters," *IEEE Trans. Power Electron.*, vol. 30, no. 4, pp. 1836–1842, Apr. 2015.

[13] A. Edpuganti and A. K. Rathore, "Optimal pulsewidth modulation of medium-voltage modular multilevel converter," *IEEE Trans. Ind. Appl.*, vol. 52, no. 4, pp. 3435–3442, Jul. 2016.

[14] A. Dekka, B. Wu, and N. R. Zargari, "A novel modulation scheme and voltage balancing algorithm for modular multilevel converter," *IEEE Trans. Ind. Appl.*, vol. 52, no. 1, pp. 432–443, Jan. 2016.

[15] M. Guan and Z. Xu, "Modeling and control of a modular multilevel converter-based HVDC system under unbalanced grid conditions," *IEEE Trans. Power. Electron.*, vol. 27, no. 12, pp. 4858–4867, Dec. 2012.
[16] O. Jasim and H. Q. S. Dang, "Advanced control method for VSC-HVDC systems connected to weak grids," in *Proc. 18th Eur. Conf. Power Electron. Appl. (EPE ECCE Europe)*, Karlsruhe, Germany, Sep. 2016, pp. 1–10.
[17] B. Gutierrez and S.-S. Kwak, "Modular multilevel converters (MMCs) controlled by model predictive control with reduced calculation burden," *IEEE Trans. Power Electron.*, vol. 33, no. 11, pp. 9176–9187, Nov. 2018.
[18] J. Huang, B. Yang, F. Guo, Z. Wang, X. Tong, A. Zhang, and J. Xiao, "Priority sorting approach for modular multilevel converter based on simplified model predictive control," *IEEE Trans. Ind. Electron.*, vol. 65, no. 6, pp. 4819–4830, Jun. 2018.
[19] M. H. Nguyen and S. Kwak, "Simplified indirect model predictive control method for a modular multilevel converter," *IEEE Access*, vol. 6, pp. 62405–62418, 2018.
[20] B. Li, Z. Xu, J. Ding, and D. Xu, "Fault-tolerant control of medium-voltage modular multilevel converters with minimum performance degradation under submodule failures," *IEEE Access*, vol. 6, pp. 11772–11781, 2018.
[21] M. Abdelsalam, M. I. Marei, and S. B. Tennakoon, "An integrated control strategy with fault detection and tolerant control capability based on capacitor voltage estimation for modular multilevel converters," *IEEE Trans. Ind. Appl.*, vol. 53, no. 3, pp. 2840–2851, May/Jun. 2017.
[22] S. Yang, P. Wang, Y. Tang, M. Zagrodnik, X. Hu, and K. J. Tseng, "Circulating current suppression in modular multilevel converters with even-harmonic repetitive control," *IEEE Trans. Ind. Appl.*, vol. 54, no. 1, pp. 298–309, Jan. 2018.
[23] X. Yang, Z. Li, T. Q. Zheng, X. You, and P. Kobrle, "Virtual impedance sliding mode control-based MMC circulating current suppressing strategy," *IEEE Access*, vol. 7, pp. 26229–26240, 2019.
[24] L. Ben-Brahim, A. Gastli, M. Trabelsi, K. A. Ghazi, M. Houchati, and H. Abu-Rub, "Modular multilevel converter circulating current reduction using model predictive control," *IEEE Trans. Ind. Electron.*, vol. 63, no. 6, pp. 3857–3866, Jun. 2016.
[25] F. Ma, Q. Xu, Z. He, C. Tu, Z. Shuai, A. Luo, and Y. Li, "A railway traction power conditioner using modular multilevel converter and its control strategy for high-speed railway system," *IEEE Trans. Transport. Electrific.*, vol. 2, no. 1, pp. 96–109, Mar. 2016.
[26] Q. Xu, F. Ma, Z. He, Y. Chen, J. M. Guerrero, A. Luo, Y. Li, and Y. Yue, "Analysis and comparison of modular railway power conditioner for high-speed railway traction system," *IEEE Trans. Power Electron.*, vol. 32, no. 8, pp. 6031–6048, Aug. 2017.
[27] M. Tanta, V. Monteiro, B. Exposto, J. G. Pinto, A. P. Martins, A. S. Carvalho, A. A. N. Meléndez, and J. L. Afonso, "Simplified rail power conditioner based on a half-bridge indirect AC/DC/AC modular multilevel converter and a V/V power transformer," in *Proc. 43rd Annu. Conf. IEEE Ind. Electron. Soc. (IECON)*, Beijing, China, Oct./Nov. 2017, pp. 6431–6436.
[28] X. He, P. Han, M. Zhu, S. Gao, X. He, S. Gao, and W. Peng, "Advanced traction power supply system based on modular multilevel converters," in *Proc. Asian Conf. Energy, Power Transp. Electrific. (ACEPT)*, Singapore, Oct./Nov. 2018, pp. 1–8.
[29] O. F. Kececioglu, H. Acikgoz, A. Gani, and M. Sekkeli, "Experimental investigation on buck converter using neuro—Fuzzy controller," *Int. J. Intell. Syst. Appl. Eng.*, vol. 7, no. 1, pp. 1–6, Mar. 2019.
[30] O. F. Kececioglu, "Dynamic performance comparison of LQR and LQI controllers on buck converter," *Int. Congr. Eng. Archit.*, Alanya, Turkey, Nov. 2018, pp. 1904–1918.
[31] O. F. Kececioglu, "Robust control of buck converter using PI-fuzzy controller," *Int. Congr. Eng. Archit.*, Alanya, Turkey, Nov. 2018, pp. 1919–1928.

XIAOQIONG HE (M'18) received the B.Sc. and D.Eng. degrees in electrical engineering from Southwest Jiaotong University (SWJTU), Chengdu, China, in 1998 and 2013, respectively. She joined the SWJTU as a Teaching Assistant, in 1999, where she was a Lecturer, from 2003 to 2008. She is currently an Associate Professor with the School of Electrical Engineering, SWJTU. Her research interests include applications to power electronic converters, active power filters, and PWM rectifiers.

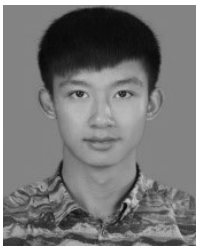

JUN PENG (S'19) was born in Chengdu, China, in 1995. He received the B.S. degree in electrical engineering from Southwest Jiaotong University, Chengdu, China, in 2018, where he is currently pursuing the M.S. degree. His research interests include modular multilevel converters, APF, and advanced traction power supply systems.

PENGCHENG HAN (S'18) was born in Henan, China, in 1992. He received the B.Sc. degree in electrical engineering from Southwest Jiaotong University (SWJTU), Chengdu, China, in 2015, where he is currently pursuing the Ph.D. degree in electrical engineering. His research interests include multilevel converters, electrified railways, control applications to power electronic converters, and SiC devices and control. His article *Fault Diagnosis and System Reconfiguration Strategy of Single-phase Cascaded Inverter* has received the Best Paper Award from the IEEE ITEC Asia–Pacific and the IEEE Industry Application Society, in 2017.

ZI LIU was born in Anhui, China, in 1995. He received the B.S. degree in electrical engineering from Southwest Jiaotong University, Chengdu, China, in 2019, where he is currently pursuing the M.S. degree in electrical engineering. His research interests include cascaded converters, the control of PWM rectifiers, and advanced traction power supply systems.

SHIBIN GAO received the B.S., M.S., and Ph.D. degrees in electrical engineering from Southwest Jiaotong University (SWJTU), Chengdu, China, in 1986, 1999, and 2006, respectively.

He is currently a Professor with the SWJTU. His current research interest includes protection and control of electric traction systems.

PENG WANG received the B.Sc. degree in electrical engineering from Xi'an Jiaotong University, Xi'an, China, in 1978, the M.Sc. degree in electrical engineering from the Taiyuan University of Technology, Taiyuan, China, in 1987, and the M.Sc. and Ph.D. degrees in power engineering from the University of Saskatchewan, Saskatoon, Canada, in 1995 and 1998, respectively.

He is currently a Full Professor with Nanyang Technological University, Singapore.